International Conference on Space Optics—ICSO 2022

Dubrovnik, Croatia

3–7 October 2022

Edited by Kyriaki Minoglou, Nikos Karafolas, and Bruno Cugny,

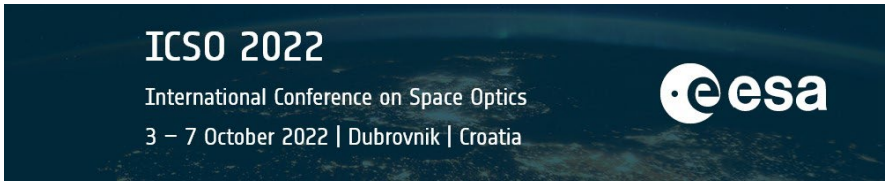

First Experimental Demonstration of Optical Feeder Link by Using the Optical Data Relay Satellite "LUCAS"

International Conference on Space Optics — ICSO 2022, edited by Kyriaki Minoglou, Nikos Karafolas, Bruno Cugny, Proc. of SPIE Vol. 12777, 127770U · © 2023 ESA and CNES · 0277-786X · doi: 10.1117/12.2689017

First Experimental Demonstration of Optical Feeder Link by Using the Optical Data Relay Satellite "LUCAS"

Hideaki Kotake*[a], Yuma Abe[a], Yasuhiro Takahashi[a], Takuya Okura[a], Tetsuharu Fuse[a],
Yohei Sato[b], Takamasa Itahashi[b], Shiro Yamakawa[b] and Morio Toyoshima[a]
[a]National Institute of Information and Communications Technology,
4-2-1 Nukui-Kitamachi, Koganei, Tokyo, 184-8795, Japan
[b]Japan Aerospace Exploration Agency,
2-1-1 Sengen, Tsukuba-shi, Ibaraki, 305-8505, Japan
*h.kotake@nict.go.jp

Abstract

In this paper, we present first results in the experimental demonstration campaign of optical feeder link conducted in November 2021, by using the Laser Utilizing Communication System (LUCAS) onboard the optical data relay GEO satellite. This campaign has been worked under the collaboration for both the National Institute of Information and Communications Technology (NICT) and the Japan Aerospace Exploration Agency (JAXA). In our experiment, we utilize the optical ground station with 1 meter telescope, which is installed in the Okinawa Electromagnetic Technology Center of NICT. This paper mainly discuss received optical power, acquisition and tracking performance, bit error rate performance of the downlink and received optical power of the uplink in an optical feeder link.

Keywords: Geostationary Earth Orbit (GEO) Satellite, Laser Utilizing Communication System (LUCAS), Optical Feeder Link, Atmospheric Turbulence, Received Optical Power, Acquisition and Tracking, Bit Error Rate (BER)

1. INTRODUCTION

Laser satellite communication has attracted much attention to increase the channel capacity of satellite communication systems. Some companies and organizations have been proceeding the research and development for laser satellite communications worldwide. Furthermore, laser satellite communication experiments were demonstrated for inter-satellite optical link missions and ground-to-satellite optical link missions in the past [1].

Inter-satellite optical links, which utilize geostationary earth orbit (GEO) satellites, have been operated as the optical data relay missions. The European Space Agency (ESA) launched the European Data Relay System (EDRS) and started operating the data relay service by utilizing two low earth orbit (LEO) satellites [2]. The National Aeronautics and Space Administration (NASA)also launched the Laser Communication Relay Demonstration (LCRD) and started operation of the data relay system in December 2021 [3,4]. In Japan, the Japan Aerospace Exploration Agency (JAXA) launched optical data relay GEO satellite called as the Laser Utilizing Communication System (LUCAS) in November 2020 [5,6]. They will conduct inter-satellite optical link demonstrations between the GEO satellite and LEO satellites. Therefore, inter-satellite optical link has been approaching into practical use.

Ground-to-satellite optical link experiments have also been demonstrated on the LEO orbits such as the Small Optical TrAnsponder (SOTA) developed by the National Institute of Information and Communications Technology (NICT) [7] and the Small Optical Link for International Space Station (SOLISS) developed by Sony Computer Science Laboratories (Sony CSL) [8]. However, since clouds and atmospheric turbulences interrupt the communication performances between ground and satellites, ground-to-satellite laser communications still have a difficult challenge for practical use. In order to provide a stable ground-to-satellite laser communications, the effects of atmospheric turbulences, which include receiver power fluctuations, tracking error and bit error rate, need to be surveyed for optical system design of ground-to-satellite laser communication links.

Under the scenarios, NICT started the experimental demonstration of optical feeder link using the LUCAS under the collaborative work with JAXA. The optical feeder link, which implements bidirectional ground-to-GEO satellite optical links, has been established between the LUCAS and optical ground station (OGS) installed in the Okinawa Electromagnetic Technology Center of NICT (called as NICT Okinawa), Japan. OGS implements the check-out equipment and 1 meter telescope for optical communications. Furthermore, a custom photo detector module with 5

centimeters telescope for measurement of received optical power is implemented on the OGS. We conducted the measurement and analysis of the effects of atmospheric turbulences and communication performances of laser communications at a wavelength of 1.5 micrometers in the ground-to-GEO satellite optical links. We will proceed for the practical use of optical feeder link by utilizing the experimental data. In addition, ground-to-GEO satellite optical link experiment has been demonstrated since the optical link experiment using the Laser Communication Equipment (LCE) onboard the Engineering Test Satellite-VI (ETS-VI) conducted from 1994 to 1996 [9].

This paper is organized as follows. The overview of LUCAS is described in Section 2. The experimental setup and conditions of the demonstration for optical feeder link are presented in Section 3. The experimental results, which include received optical power, acquisition and tracking performance and bit error rate related with the atmospheric turbulences, will be discussed in Section 4. The conclusions are finally remarked in Section 5.

2. LASER UTILIZING COMMUNICATION SYSTEM "LUCAS"

Optical data relay GEO satellite called as the Laser Utilizing Communication System (LUCAS) was developed as a next-generation data relay system by JAXA. The LUCAS was launched by H-ⅡA rocket in November 2020 [5,6,10]. The LUCAS has the novel function to transmit and receive a large volume of data between GEO satellite and LEO satellite by inter-satellite optical links. Figure 1 shows an image of optical data relay satellite called as the LUCAS.

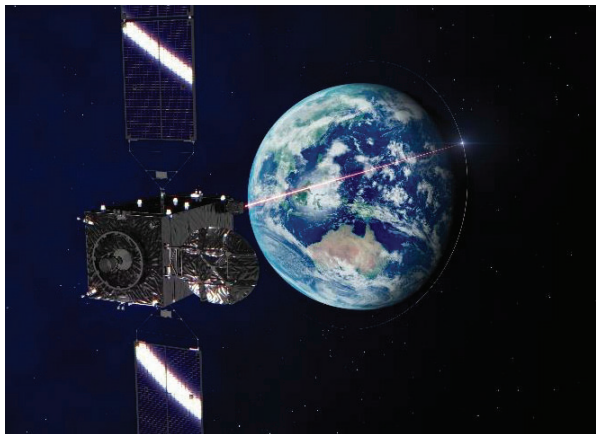

Figure 1. Image of optical data relay satellite called as the LUCAS [5,6]

Table 1 shows the primary technical specifications. Return link denotes an optical communication link from LEO satellite to GEO satellite called as the LUCAS. It enables transmissions of earth observation image data captured by LEO satellite. Forward link denotes an optical communication link from the LUCAS to LEO satellite. It enables transmissions of control data for LEO satellite. For that reason, different data rate and modulation are utilized for several purposes in each link.

After the LUCAS was launched, initial in-orbit check-out was conducted from January to February in 2021. Initial in-orbit check-out includes the function and performance evaluation work. In the check-out, we verified the acquisition, tracking and pointing (ATP) function of LUCAS utilizing OGS installed in NICT Okinawa. The OGS is also regarded as an actual LEO satellite in this work. Figure 2 illustrates the images before and after the establishment of tracking, captured by an infrared camera. Both images indicate that optical signal from the satellite is strongly received after the tracking. As a result, we confirmed that bidirectional optical links could be established by the ATP function of the LUCAS.

Currently, after the LUCAS received earth observation image data from LEO satellite, the LUCAS transmits the data to radio frequency (RF) ground station via RF feeder link. In the future, we aim at utilizing an optical feeder link instead of RF feeder link. Under the scenarios, we started the measurement and analysis of the effects of atmospheric turbulences

and communication performances of ground-to-GEO satellite optical links, in order to practically use an optical feeder link.

Table 1. Primary technical specification of the LUCAS [10].

User data rate	Return link: 1.8 Gbps Forward link: 50 Mbps
Optical wavelength	1550 nm
Modulation method	Return link: RZ-DPSK-DD Forward link: IM-DD
Satellite available for communications	LEO satellite Altitude: 200-1000km

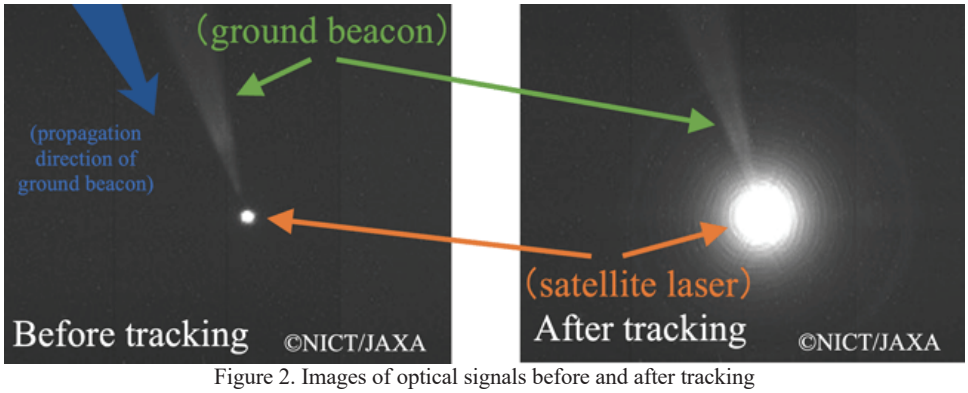

Figure 2. Images of optical signals before and after tracking

3. GROUND-TO-SATELLITE OPTICAL LINK EXPERIMENT

3.1 Experimental setups

Figure 3 illustrates the experimental setup of ground-to-satellite optical link experiment by using the LUCAS with 14 centimeters optical antenna. Ground-to-satellite optical links, which implements downlink and uplink, can be established between the LUCAS and the OGS installed in NICT Okinawa by a series of acquisition and tracking sequences. The LUCAS exists within the range of the elevation angle between 35 degrees and 42 degrees from the corresponding OGS. The LUCAS outputs about 60 Mbps downlink optical signal to the OGS. The downlink optical signals are received by the check-out equipment via 1 meter telescope in the OGS. The data rate of 60 Mbps includes user data length and forward error correction (FEC) code length. The check-out equipment outputs 2.5Gbps uplink optical signal from the OGS to the LUCAS. The uplink optical signals are received by LUCAS. The data rate of 2.5 Gbps also includes user data length and FEC code length. In our BER performance evaluation, LUCAS forwards the PN (Pseudo random Noise) code to the OGS instead of using FEC code.

Figure 4(a) describes the experimental setup around 1 meter telescope inside the OGS installed in NICT Okinawa, and Figure 4(b) shows the block diagram of the check-out equipment. The telescope condenses the downlink optical signals onto the check-out equipment and transmits the uplink optical signals generated from the check-out equipment. The downlink optical signal is received by the ATP function and optical receiver of the check-out equipment. The uplink optical signal is transmitted by ATP function and optical transmitter of the check-out equipment. An IR (Infrared) camera is implemented on the right side of 1 meter telescope. The IR camera captures the images of the downlink and uplink optical signals. A custom photo detector module with 5 centimeters is implemented on the left side of 1 meter

telescope. The photo detector module measures the received optical power of the downlink optical signals by using 5 centimeters telescope. Differential image motion monitor (DIMM) device is implemented on the lower side of 1 meter telescope. The DIMM device measures many images of received downlink optical signals to analyze Fried parameter that is one of parameters for atmospheric turbulences. The analytical results of Fried parameter will be discussed in another paper [11].

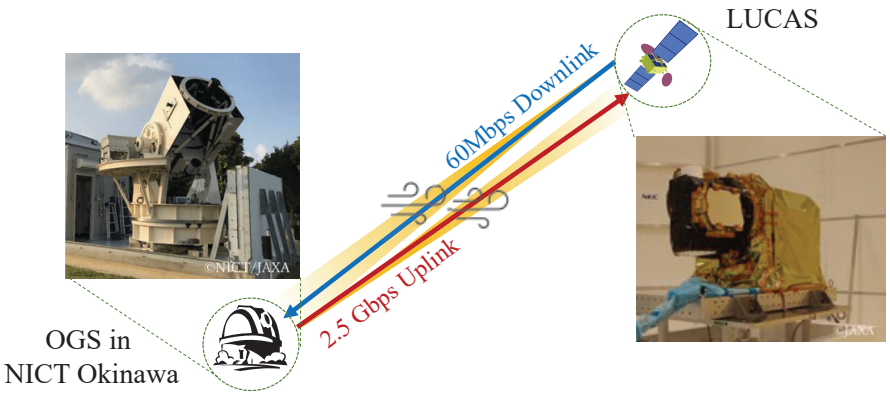

Figure 3. Experimental setup of ground-to-satellite optical link experiment by using LUCAS and OGS installed in NICT Okinawa

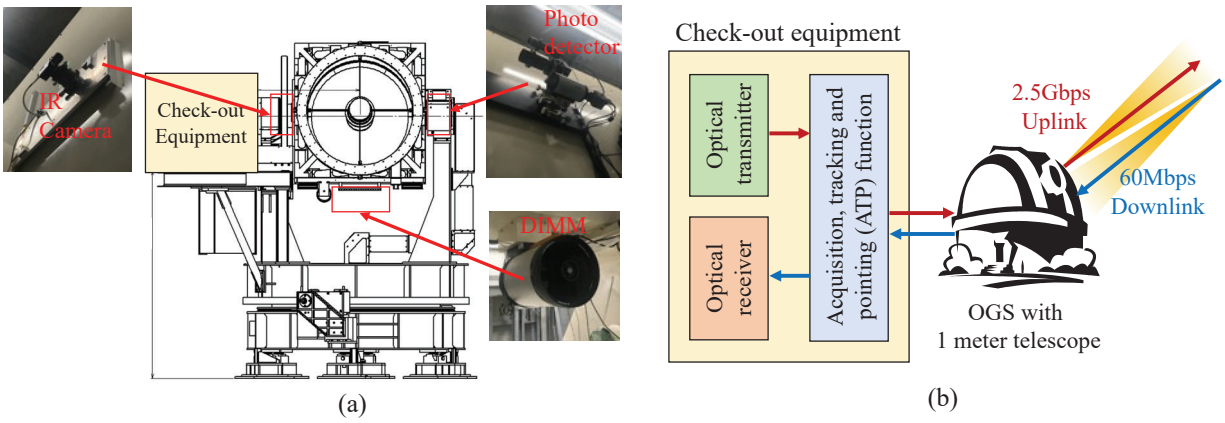

Figure 4. (a) Experimental setup around 1 meter telescope inside the OGS installed in NICT Okinawa and (b) the block diagram of the check-out equipment

3.2 Experimental conditions

We conducted the trial campaign of acquisition and tracking of 83 times at the night in November 2021. We successfully demonstrated the acquisition and tracking trials of 35 times in the campaign. In each unsuccessful case, the acquisition and tracking has mainly not been completed by climates and clouds. In other cases, we have not confirmed technical issues for LUCAS. In this paper, we select three cases including (a) stable, (b) moderate and (c) unstable cases for the downlink among the successful cases of acquisition and tracking from the viewpoint of received optical power and fade duration. We also select two cases for the uplink in the successful cases of acquisition and tracking. The measurement duration of each case is 20 seconds. Table 2 shows experimental environmental conditions of each case in the experimental demonstration campaign. The environmental data has been captured by Observation system of the patch of Blue Sky for Optical Communication (OBSOC) [12].

Table 2. Experimental environmental conditions in the experimental demonstration campaign.

Case	Downlink			Uplink	
	(a)Stable	(b)Moderate	(c)Unstable	(a)	(b)
Month/Day	Day 12th, November	Day 13th, November	Day 16th, November	Day 12th, November	Day 12th, November
Visibility	Clear, sometimes cloudy	Clear	Clear	Clear, sometimes cloudy	Clear
Time	20:50:33	1:56:28	23:47:18	20:50:40	23:19:40
Temperature [℃]	19.6	18.9	20.3	19.6	18.9
Humidity [%]	52.9	53	62.4	53.3	52.9
Pressure [hPa]	1020.22	1018.62	1018.94	1020.22	1019.8
Wind velocity [m/s]	0.5	1.8	1.3	0.8	0.1
Wind direction [deg]	292.5	45	67.5	67.5	45

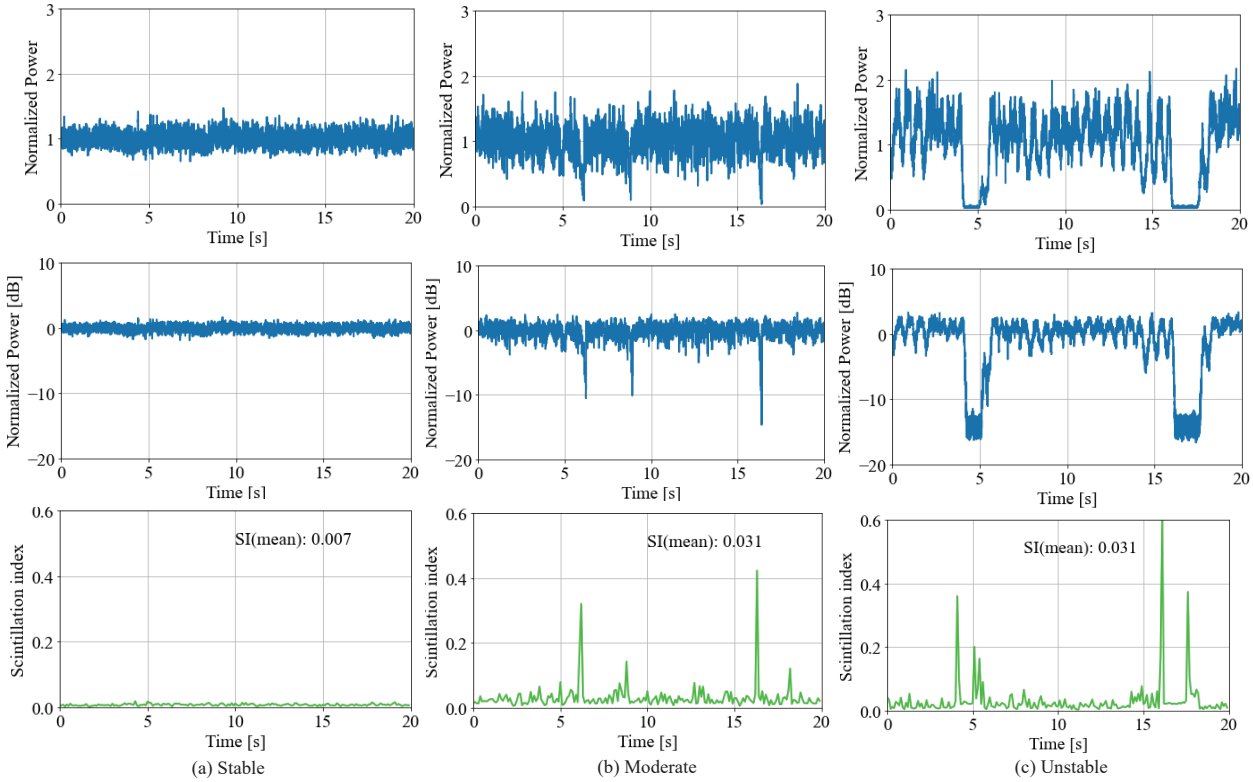

Figure 5. Received optical power and SI of the downlink, measured by the check-out equipment with 1 meter telescope in three cases including (a) stable (b) moderate and (c) unstable cases

4. EXPERIMENTAL RESULTS

4.1 Received optical power and scintillation index in the downlink and the uplink

Figure 5 shows received optical power and scintillation index (SI) of the downlink, measured by fast pointing sensor (FPS) of the ATP function of the check-out equipment with 1 meter telescope in three cases including (a) stable, (b) moderate and (c) unstable cases. Figure 6 also shows received optical power and SI of the downlink, measured by the

custom photo detector module with 5 centimeters telescope in three cases including (a) stable, (b) moderate and (c) unstable cases. Received optical power has been measured at a sampling frequency of a few kHz. It is normalized by using received optical power averaged in the measurement span and is shown as the blue line. SI, which is calculated at the time interval of 0.1 second by using the equation expressed in [13], is also shown as the green line.

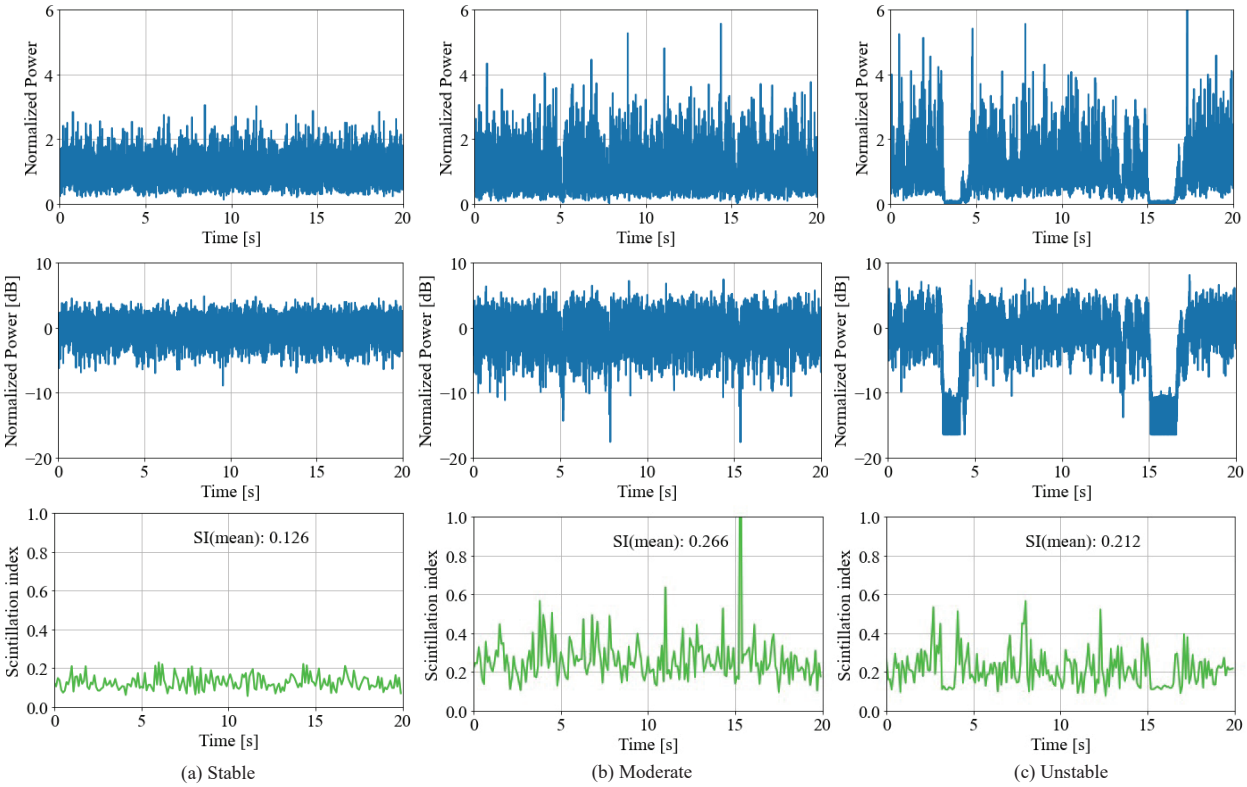

Figure 6. Received optical power and SI of the downlink measured by the custom photo detector module with 5 centimeters telescope in three cases including (a) stable (b) moderate and (c) unstable cases

From Figure 5(a), it can be seen that received optical power keeps stable at the center of average optical power and SI is also suppressed to the lowest value. As shown in Figure 5(b), it appears that SI of (b) moderate case is higher than that of (a) stable case and instantaneous fades of received optical power occasionally happen. Figure 5(c) presents the long fade duration caused by fades of received optical power in (c) unstable case. Thus, we can say that received optical power and SI have different characteristics in each case.

Furthermore, we compare received optical power and SI in each case, by using experimental environmental conditions listed in Table 2. It can be inferred that the wind speed may cause the strong power fluctuations, according to the results of (a) stable case and (b) moderate case. The results also predict that the humidity may cause the strong power fluctuations. However, little still may not be clear about the relationship between received optical power fluctuations and environmental conditions from these results only. In order to clarify such relationship, we need to evaluate and analyze experimental data continuously.

Both Figure 5 and Figure 6 show that received optical power and SI have the same trends in both telescopes. However, it can be seen that received optical power and SI with 5 centimeters telescope fluctuates more strongly than with 1 meter telescope. The results show that the aperture averaging effect caused by 1 meter telescope enable decreasing SI.

Consequently, we clarified that a large-aperture size telescope can contribute to the suppression of received optical power fluctuations.

Figure 7 shows received optical power and scintillation index (SI) of the uplink, measured by the FPS of the ATP function of the LUCAS with 14 centimeters optical antenna in two cases including both (a) case and (b) case. Received optical power was measured at a sampling frequency of about 100 Hz. It is normalized by using received optical power averaged in the measurement span and is shown as the blue line. SI, which is calculated at the time interval of 0.1 second, is also shown as the green line.

According to Figure 5 and Figure 7, received optical power and SI with 1 meter telescope of OGS fluctuate more strongly than those with 14 centimeters telescope of LUCAS. From these results, since the optical aperture of LUCAS is smaller than that of OGS, it is considered that aperture averaging effect is decreased to the low value. Furthermore, according to Figure 6 and Figure 7, despite the optical aperture of LUCAS is larger than that of the custom photo detector module with 5 centimeters telescope, received optical power and SI in the uplink fluctuates more strongly than in the downlink. These results predict that the strength of atmospheric turbulence in the uplink is stronger than in the downlink. It needs to be investigated in more detail.

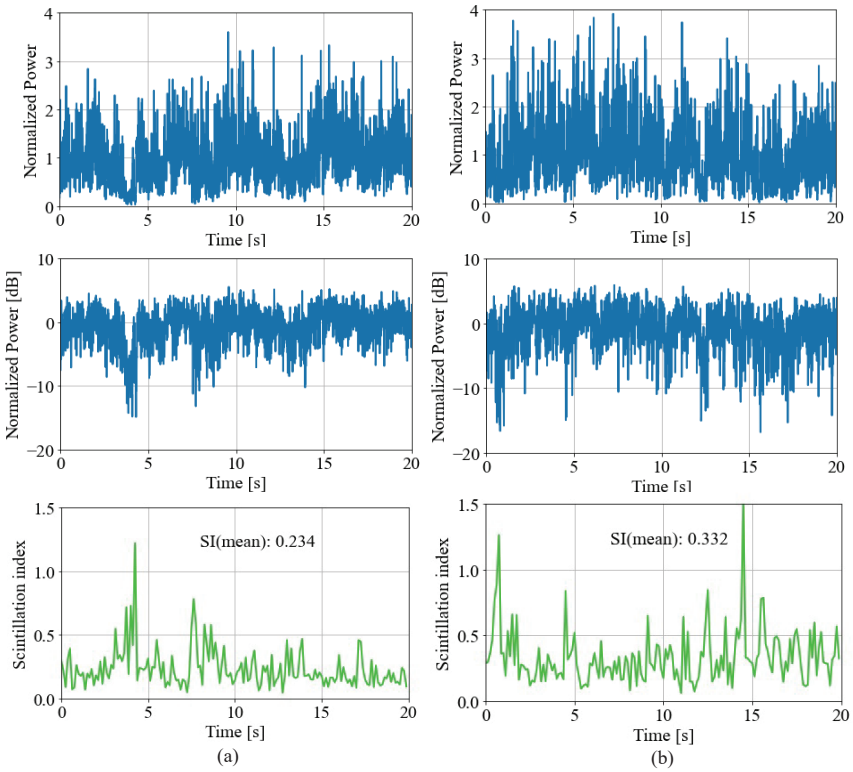

Figure 7. Received optical power and SI of the uplink, measured by the LUCAS with 14 centimeters optical antenna in two cases including both (a) case and (b) case

4.2 Acquisition and tracking performance in the downlink

Figure 8 shows tracking error of the downlink in both axes (X, Y), measured by the FPS of the ATP function of the check-out equipment with 1 meter telescope in three cases including (a) stable (b) moderate and (c) unstable cases. Tracking error has been measured as the acquisition and tracking performance in the unit of urad at a sampling frequency

of a few kHz. It is shown as the blue line. Tracking errors, which are averaged at the time interval of 0.1 second in both axes, are also shown as the orange line. Means of absolute value of tracking error are displayed in each graph.

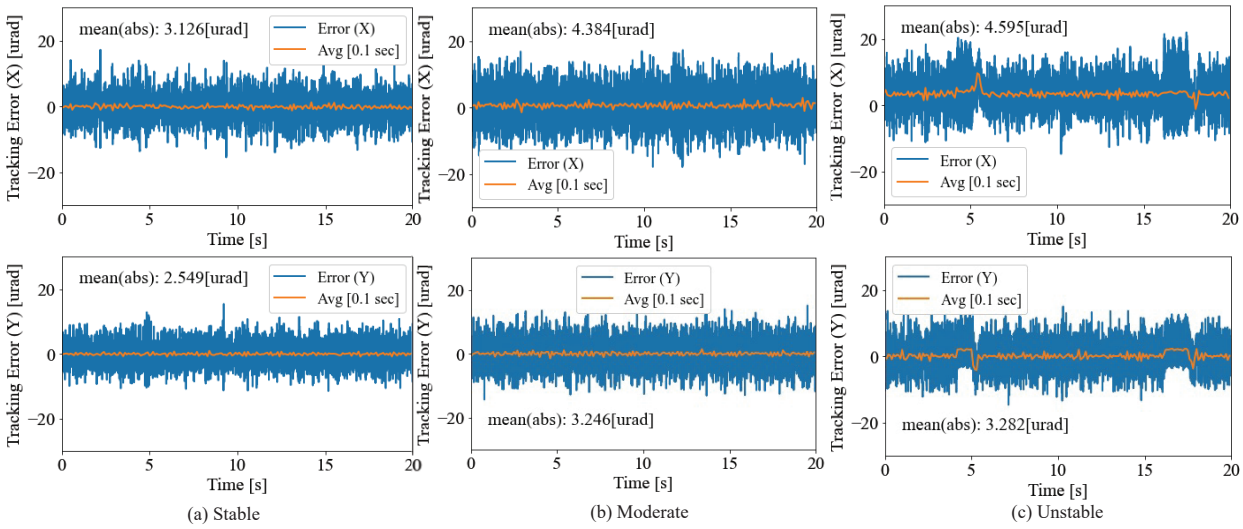

Figure 8. Tracking error of the downlink, measured by the check-out equipment with 1 meter telescope in three cases including (a) stable (b) moderate and (c) unstable cases

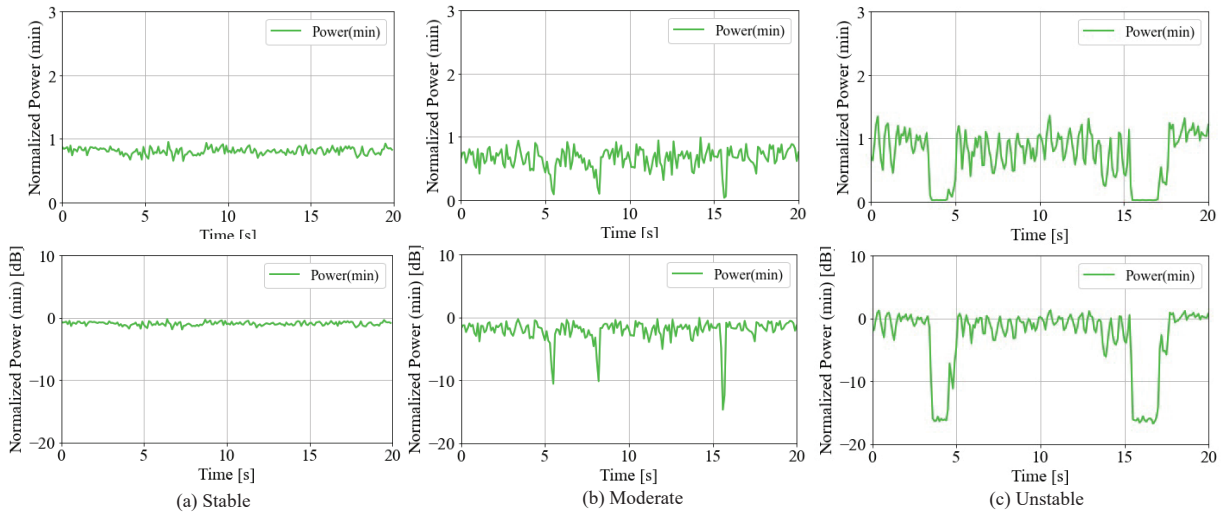

Figure 9. Minimum received optical power of the downlink, measured by the check-out equipment with 1 meter telescope in three cases including (a) stable (b) moderate and (c) unstable cases

According to Figure 8(a), tracking error keeps stable at the center of 0 urad in both axes and mean of absolute value of tracking error is also suppressed to the lower value. It can also be confirmed that the distribution of tracking error becomes broadened at the center of 0 urad in both axes in Figure 8(b). Both Figure 8(a) and Figure 8(b) indicates that mean of absolute value of tracking error in (a) stable case is higher than in (b) moderate case. As depicted in Figure 8(c),

we can find that the center value of tracking error increases in X axis and mean of absolute value of tracking error also reaches to the highest value in each case. Compared with received optical power described in Figure 5(c), tracking error largely varies at the timing of fades. Therefore, it is clearly found that received optical power and tracking error have the mutual relationship.

4.3 Bit error rate performance in the downlink

Figure 9 shows the minimum received optical power of the downlink, measured by the FPS of the ATP function of the check-out equipment with 1 meter telescope in three cases including (a) stable (b) moderate and (c) unstable cases. Figure 10 shows the bit error rate (BER) performance of the downlink, measured by the check-out equipment. We have defined minimum value of received optical power sampled at a few of kHz frequency at the time interval of about 100 milli-seconds as minimum received optical power. It is normalized by using received optical power averaged in the measurement span and is shown as the green line. BER has been measured at the time interval of about 0.1 second in each case.

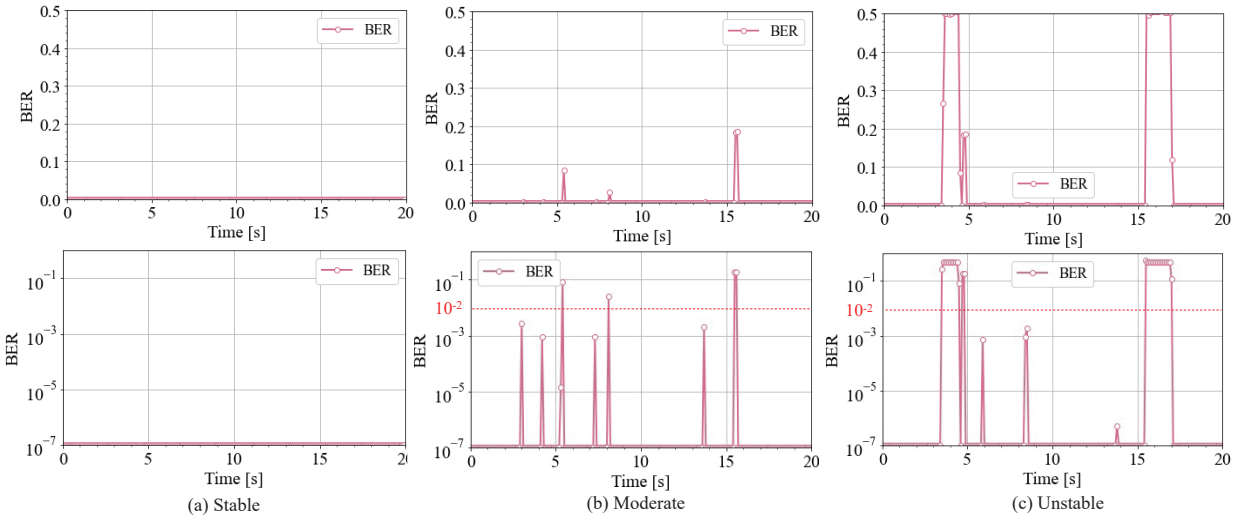

Figure 10. BER performance of the downlink, measured by the check-out equipment with 1 meter telescope in three cases including (a) stable (b) moderate and (c) unstable cases

Figure 10(a) indicates that BER reaches to error free. The main reason is the low fluctuations of minimum power illustrated in Figure 9(a). Despite minimum received optical power illustrated in Figure 9(b) is relatively stable, BER occurs at several times. Moreover, when normalized power is lower than -10dB in Figure 9(b), BER becomes higher than 10^{-2}. It can be confirmed that BER instantaneously increases due to the rapid change of received optical power. Furthermore, as shown in Figure 10(c), some continuous fades of received optical power described in Figure 9(c) cause to the burst error.

Consequently, we can clarify that there is a relationship between minimum received optical power described in Figure 9 and BER described in Figure 10. These results present that atmospheric conditions can be estimated at some level as BER is monitored. However, it can be found from the log-scale graph depicted in Figure 10 that BER sometimes increases to 10^{-3} at the timing point when minimum received optical power slightly change. It can be inferred that BER needs to be measured at higher sampling frequency that is higher than about 10 Hz in order to monitor accurate atmospheric conditions from BER. Thus, the fast sampled BER monitoring function needs to be considered in the development of next-generation ground-to-satellite optical communication systems.

5. CONCLUSIONS

In this paper, we present first experimental demonstration results of optical feeder link conducted in November 2021, by using the LUCAS onboard the optical data relay GEO satellite. Especially, we select three cases among the successful cases of acquisition and tracking and mainly discuss received optical power, acquisition and tracking performance, bit error rate performance of the downlink and received optical power of the uplink in an optical feeder link. As a result, we can clarify that received optical power of each case shows various characteristics, depending on atmospheric environmental conditions in the downlink. It is also suggested that the strength of atmospheric turbulence of the downlink is stronger than that of the uplink. In addition, it appears that acquisition and tracking performance and BER performance are closely related with received optical power of each case in the downlink. It is also found that the fast sampled monitoring is important to monitor accurate atmospheric conditions from BER in the future ground-to-satellite optical communication system.

In the future works, we are going to proceed the detailed analysis of atmospheric turbulences for ground-to-GEO satellite optical link and investigate and the relationship with some kinds of environmental data. Furthermore, we will investigate the trends of atmospheric turbulences for all seasons.

ACKNOWLEDGEMENTS

The authors would like to thank NEC Corporation, Nishimura Co. Ltd, and Space Engineering Development Co. Ltd. for their continuous support for the check-out and the operations of ground-to- satellite optical link experiments by using LUCAS and OGS installed in the Okinawa Electromagnetic Technology Center of NICT.

REFERENCES

[1] M. Toyoshima, “Recent Trends in Space Laser Communications for Small Satellites and Constellations,” IEEE J. Lightwave Tech., vol.39, No.3, pp.693-699, 2021.
[2] F. Heine et al., “Status of Tesat laser communication activities,” Proc. SPIE, 1127204, 2020.
[3] B. L. Edwards et al., “An overview of NASA’s latest effort in optical communications,” IEEE International Conference on Space Optical Systems and applications (ICSOS), pp.1-8, 2015.
[4] B. L. Edwards et al., “Challenges, Lessons Learned, and Methodologies from the LCRD Optical Communication System AI&T,” IEEE International Conference on Space Optical Systems and applications (ICSOS), a7, 2022.
[5] S. Yamakawa et al., “JAXA’s Optical Data Relay Satellite Programme,” IEEE International Conference on Space Optical Systems and applications (ICSOS), pp.1-3, 2015.
[6] S. Yamakawa et al., “LUCAS: The second-generation GEO satellite-based space data-relay system using optical link,” IEEE International Conference on Space Optical Systems and applications (ICSOS), a4, 2022.
[7] H. Takenaka et al., “In-orbit verification of small optical transponder (SOTA): evaluation of satellite-to-ground laser communication links,” Proc. SPIE, 973903, 2016.
[8] K. Iwamoto et al., “Experimental results on in-orbit technology demonstration of SOLISS,” Proc. SPIE, 116780D, 2021.
[9] K. Araki et al., “Experimental operations of laser communication equipment onboard ETS-VI satellite,” Proc. SPIE, 2990, 1997.
[10] https://www.satnavi.jaxa.jp/ja/project/lucas/index.html
[11] Y. Abe et al., “Preliminary DIMM-Based Analysis of Atmospheric Turbulence by Using Optical Data Relay Satellite "LUCAS",” International Conference on Space Optics (ICSO), 2022 (to be published).
[12] K. Suzuki et al., ‘Environmental-data Collection System for Satellite-to-Ground Optical Communications', Trans. JSASS Aerospace Tech. Japan, Vol.16, No.1, pp.35-39, 2018-02.
[13] D. R. Kolev et al., “Received-Power Fluctuation Analysis for LEO Satellite-to-Ground Laser Links,” IEEE J. Lightwave Tech., vol.35, No.1, pp.103-112, 2017.